Griffithsin and Carrageenan Combination To Target Herpes Simplex Virus 2 and Human Papillomavirus

Keith Levendosky,[a] Olga Mizenina,[a] Elena Martinelli,[a] Ninochka Jean-Pierre,[a]* Larisa Kizima,[a] Aixa Rodriguez,[a] Kyle Kleinbeck,[a] Thierry Bonnaire,[a] Melissa Robbiani,[a] Thomas M. Zydowsky,[a] Barry R. O'Keefe,[b] José A. Fernández-Romero[a]

Center for Biomedical Research, Population Council, New York, New York, USA[a]; Molecular Targets Laboratory, Center for Cancer Research, NCI at Frederick, Frederick, Maryland, USA[b]

Extensive preclinical evaluation of griffithsin (GRFT) has identified this lectin to be a promising broad-spectrum microbicide. We set out to explore the antiviral properties of a GRFT and carrageenan (CG) combination product against herpes simplex virus 2 (HSV-2) and human papillomavirus (HPV) as well as determine the mechanism of action (MOA) of GRFT against both viruses. We performed the experiments in different cell lines, using time-of-addition and temperature dependence experiments to differentiate inhibition of viral attachment from entry and viral receptor internalization. Surface plasmon resonance (SPR) was used to assess GRFT binding to viral glycoproteins, and immunoprecipitation and immunohistochemistry were used to identify the specific glycoprotein involved. We determined the antiviral activity of GRFT against HSV-2 to be a 50% effective concentration (EC_{50}) of 230 nM and provide the first evidence that GRFT has moderate anti-HPV activity (EC_{50} = 0.429 to 1.39 μM). GRFT blocks the entry of HSV-2 and HPV into target cells but not the adsorption of HSV-2 and HPV onto target cells. The results of the SPR, immunoprecipitation, and immunohistochemistry analyses of HSV-2 combined suggest that GRFT may block viral entry by binding to HSV-2 glycoprotein D. Cell-based assays suggest anti-HPV activity through α_6 integrin internalization. The GRFT-CG combination product but not GRFT or CG alone reduced HSV-2 vaginal infection in mice when given an hour before challenge (P = 0.0352). While GRFT significantly protected mice against vaginal HPV infection when dosed during and after HPV16 pseudovirus challenge (P < 0.026), greater CG-mediated protection was afforded by the GRFT-CG combination for up to 8 h (P < 0.0022). These findings support the development of the GRFT-CG combination as a broad-spectrum microbicide.

Griffithsin (GRFT), a lectin with a high affinity for mannose-rich N-linked glycans, has recently been identified to be a potent and broad-spectrum antiviral agent. GRFT is one of the most potent agents against human immunodeficiency virus (HIV), having 50% effective concentrations (EC_{50}s) in the low-picomolar range (1). The anti-HIV activity of GRFT, which is even better than that of other promising lectins (2), has prompted the development of GRFT as a microbicide candidate to prevent HIV acquisition. Its mechanism of action (MOA) is well characterized, targeting viral entry by binding to high-mannose oligosaccharides on gp120. GRFT does not impede binding of HIV to CD4 but, rather, prevents gp120 interaction with HIV coreceptors (3). The dimeric nature of GRFT, with three carbohydrate-binding sites per monomer, may result in HIV aggregation via multivalent interactions between GRFT and gp120 oligosaccharides (4). In addition to its potent anti-HIV activity, GRFT shows a favorable safety profile (1, 5, 6). GRFT has potent antiviral activity against the agents causing other sexually transmitted infections (STIs), like herpes simplex virus 2 (HSV-2) (7) and hepatitis C virus (HCV) (8). A large-scale method to produce GRFT in tobacco plants has been developed (1).

Carrageenan (CG), a sulfated polysaccharide extracted from seaweeds, is probably the most potent known anti-human papillomavirus (anti-HPV) agent described in preclinical studies (9–12). CG is generally recognized as safe (GRAS) by the Food and Drug Administration (FDA), and several clinical trials have shown that CG-containing gels are safe and acceptable for vaginal application (13–16). Marais et al. showed that the vaginal application of a CG-based formulation in highly compliant subjects reduced HPV prevalence (17), and current phase 2b trials are looking at the anti-HPV properties of a CG-containing sexual lubricant. The

antiviral activity of CG against HSV-2 has also been previously documented (18–20), and we have shown that CG in combination with zinc acetate results in synergistic antiviral activity against HSV-2 (21).

Here, we evaluated whether the combination of GRFT and CG can be used to boost the anti-HSV-2 properties of GRFT while incorporating the potent anti-HPV activity of CG. We further explored the MOA of GRFT against HSV-2, as well as the possible antiviral activity and MOA of GRFT against HPV.

MATERIALS AND METHODS

Cells, viruses, and antiviral compounds. HeLa cells (ATCC, Rockville, MD), Vero cells (ATCC), and TZM-bl cells (NIH AIDS Research and Reference Reagent Program, Germantown, MD) were grown in Dulbecco modified Eagle medium (DMEM; Life Technologies, Grand Island, NY) supplemented with 10% heat-inactivated fetal bovine serum (FBS; Life Technologies) and with 50 U/ml of penicillin and 50 μg/ml streptomycin (Life Technologies).

The HIV-1$_{MN}$ and HIV-1$_{ADA-M}$ laboratory strains were provided by Jeffrey D. Lifson of Leidos Biomedical Research, Inc. HSV-2 strain G (ATCC) was propagated in Vero cells and the titer was determined as previously described (21). HPV16, HPV18, and HPV45 pseudoviruses (PsVs) were produced and the titers were determined as previously described (10, 12).

GRFT was produced in *Nicotiana benthamiana* as previously reported (1). The anti-HSV-2 neutralizing monoclonal antibody (MAb) DL11 (mouse anti-gD) was generously provided by Gary Cohen and Roselyn Eisenberg of the University of Pennsylvania. CG was obtained from Gelymar (Puerto Montt, Chile). The GRFT-CG combination for *in vivo* studies comprised 3% CG and 0.1% GRFT gel. The 3% CG was prepared in 10 mM sodium acetate in which the pH was adjusted to 6.8 to 7.0 with either 1 N NaOH or 1 N HCl and the osmolality was adjusted to about 250 osmol/kg with NaCl. Hydroxyethylcellulose (HEC) gel was used as a placebo in the animal models and was formulated as described by Tien et al. (22).

Antiviral activities in cell-based assays. The antiviral activity of GRFT against HIV-1 was tested using the standardized TZM-bl cell-based assay (23). The anti-HPV activities of GRFT, CG and GRFT-CG were tested in HeLa cells using the luciferase assay (10, 12).

The anti-HSV activities of GRFT, CG, and their combination were tested in Vero cells using the PrestoBlue cell viability reagent (Life Technologies). Vero cells were seeded (10^4 cells/well) in 100 μl of medium and incubated overnight at 37°C in a 5% CO_2 atmosphere with 98% humidity. Dilutions (2×) of GRFT were prepared in the appropriate dilution range. The cell culture medium on the cell monolayers was replaced with 50 μl of the diluted formulations or 50 to 100 μl of medium for virus and cell controls. Dilutions were tested in triplicate. Fifty microliters of HSV-2 G (85 PFU/well) was added to all wells with the exception of the cell controls and incubated for 6 days under standard conditions. Cell monolayers were washed with DMEM without phenol red, and then 100 μl of 1× PrestoBlue was added to each well. Fluorescence was read on a Gemini EM microplate reader (excitation and emission wavelengths, 560 nm and 600 nm, respectively).

In vitro GRFT and CG combination studies were performed using equipotent doses of GRFT, CG, or GRFT-CG (on the basis of the EC$_{50}$ for each compound). The assay for anti-HPV activity was performed as described above. Anti-HSV activity was determined using the PrestoBlue assay described above, with the only difference being that the compounds and virus were preincubated at 37°C for 6 h before they were added to the cells in order to capture better the anti-HSV-2 activity of CG. At least eight different concentrations of each compound or combination, tested in triplicate, were used to obtain dose-response curves. Cytotoxicity was estimated in all cell lines using the 2,3-bis(2-methoxy-4-nitro-5-sulfophenyl)-5-[(phenylamino)carbonyl]-2H-tetrazolium hydroxide assay (21), which mimicked the assays for antiviral activity but which did not include virus.

The antiviral activity of GRFT against HSV-2 was further evaluated using a flow cytometry assay. HeLa cells were seeded (10^4 cells/well) in 100 μl of medium and incubated overnight at 37°C in a 5% CO_2 atmosphere with 98% humidity. The cell culture medium on the cell monolayers was replaced with 50 μl of GRFT (10 and 1,000 μg/ml), 50 μl of MAb DL11 (600 μg/ml), or 50 to 100 μl of medium for virus and cell controls, followed by challenge with HSV-2 G at a multiplicity of infection (MOI) of 1 in all wells with the exception of the cell controls. The plates were incubated for 4 h at 37°C in a 5% CO_2 atmosphere with 98% humidity, and the cell monolayers were washed three times with cell culture medium, leaving 100 μl of medium per well after the last wash. The plates were incubated overnight before treatment with 100 μl of 0.25% trypsin–EDTA (Life Technologies). The cells were washed and resuspended in phosphate-buffered saline (PBS) with the live/dead discriminator Aqua for 10 min at 4°C, washed, and resuspended in Fix/Perm buffer (BD Bioscience) for 20 min at 4°C; washed and resuspended in Perm/Wash buffer with 0.5 μg of an anti-ICP-8 MAb (IgG2a isotype; Virusys, North Berwick, ME) diluted in Perm/Wash buffer for 20 min at room temperature; and washed and analyzed immediately with a BD LSRII flow cytometer. The ICP-8 MAb was directly conjugated with Alexa Fluor 647 (Zenon antibody labeling kit; Invitrogen, Life Technologies). Fifty thousand events per sample were acquired, and the results were analyzed with FlowJo software (v9).

GRFT MOA against HSV-2. (i) Inhibition of HSV-2 adsorption or entry. Vero cells were seeded in 12-well plates (2×10^4 cells/well) in 1 ml of medium and incubated overnight at 37°C in a 5% CO_2 atmosphere with 98% humidity. To study the ability of GRFT to block HSV-2 adsorption, HSV-2 G (750 PFU/ml) and different concentrations of GRFT or medium (virus control) were preincubated for 0 h, 0.5 h, and 2 h at 37°C before being added to prechilled Vero cells and kept at 4°C for 2 h. The cells were washed 3 times with prechilled culture medium, and then a methylcellulose (Fisher Scientific, Pittsburg, PA) overlay was added and the plates were incubated for 48 h at 37°C in a 5% CO_2 atmosphere with 98% humidity. Finally, the cells were fixed with 10% formalin (Sigma, St. Louis, MO) and stained with crystal violet (Sigma) to count the numbers of PFU. The same steps were performed to study entry inhibition, but after 2 h of incubation at 4°C, the cells were heated at 37°C for an additional 2 h, followed by a 2-min treatment with pH 3.0 citric acid buffer (Sigma) to inactivate any adsorbed virus particles.

(ii) Western blotting of HSV-2 lysate. Purified HSV-2 lysate (Advance Biotechnologies, Columbia, MD) was resolved in 4 to 12% bis-Tris precast gradient SDS-polyacrylamide gels (Life Technologies) and blotted onto a polyvinylidene difluoride membrane using an iBlot gel transfer system (Life Technologies). Membranes were blocked with 5% bovine serum albumin (Sigma) overnight. The blocked membranes were incubated overnight at 4°C with 1 μg/ml GRFT in PBS or with mouse anti-gD MAb DL11 diluted 1:500 in 5% nonfat instant dry milk, PBS, and 0.1% Tween. The membranes were washed and incubated with rabbit polyclonal anti-GRFT (Pacific Immunology, Ramona, CA) or anti-mouse immunoglobulin conjugated with horseradish peroxidase (HRP) (Promega, Madison, WI). After the required washing steps, the membrane used to detect GRFT binding was incubated with anti-rabbit immunoglobulin conjugated with HRP and washed again, and both membranes were processed using an enhanced chemiluminescence Western blotting detection system (Thermo Scientific).

(iii) Immunoprecipitation. Vero cells were infected with the HSV-2 G strain at an MOI of 1 and lysed 24 h or 48 h after infection. Lysis of cell pellets was performed with prechilled buffer (10^7 cells/ml) containing mild detergent (50 mM Tris-HCl, 150 mM NaCl, 1% Nonidet P-40, phenylmethylsulfonyl fluoride, pH 7.5), and the samples were kept on ice for 30 min with occasional mixing. The lysate was centrifuged at 10,000 × *g* for 15 min at 4°C, and the supernatant was collected and kept at −80°C until immunoprecipitation was performed. The supernatants were thawed and then incubated with or without GRFT (0.2 mg/ml) and primary antibodies (30 μg/ml; custom-prepared rabbit polyclonal anti-GRFT) at 4°C for 1.5 h. Controls containing only rabbit polyclonal antibody with or without GRFT were also included. Protein G beads (GE Healthcare, Pittsburgh, PA) were added to all samples, and the mixtures were rotated overnight at 4°C. The beads were collected and washed four times in ice-cold washing buffer (25 mM Tris-HCl, 150 mM NaCl, 0.05% Tween 20, pH 7.5). The samples resulting from immunoprecipitation or infected cell lysates (with which immunoprecipitation was not performed and which were used as a control for viral glycoprotein binding) were boiled with loading buffer (NuPAGE lithium dodecyl sulfate; Life Technologies) for 10 min before they were run in a 4 to 12% bis-Tris gel (Life Technol-

ogies) with MES (morpholineethanesulfonic acid) buffer (Life Technologies) at 200 V for 1 h. Western blotting was performed as described above using the following mouse monoclonal antibody configurations (all antibodies were from Virusys Corporation, Taneytown, MD): anti-HSV-2 gD (catalog number HA025) diluted 1:3,000, anti-HSV-2 gB (catalog number H1242190) diluted 1:1,500, anti-HSV-2 gH (catalog number H2A261) diluted 1:100, and anti-HSV-2 gL (catalog number H2A262) diluted 1:100 or rabbit polyclonal antibody diluted 1:400 for the GRFT controls. Anti-rabbit or anti-mouse immunoglobulin conjugated with HRP (Thermo Scientific) was used for detection.

(iv) Surface plasmon resonance (SPR). The association rate constant (k_a) and equilibrium dissociation constant (K_D) values were estimated using Bio-Rad ProteOn GLC sensor chips in a ProteOn XPR36 system (Bio-Rad, Hercules, CA). The chip surface was activated with 1-ethyl-3-(3-dimethylaminopropyl)carbodiimide hydrochloride–N-hydroxysulfosuccinimide (EDC-NHS; Bio-Rad) at 30 μl/min (flow time, 300 s), followed by glycoprotein immobilization with 0.5 μg/ml of HIV gp120 (produced in a baculovirus system and provided by ProSpec-Tany TechnoGene, Ness Ziona) or HSV-2 gD (gD-2 [306t], produced in a baculovirus system and graciously provided by Gary Cohen and Roselyn Eisenberg, University of Pennsylvania) in ProteOn acetate buffer, pH 4.5 (Bio-Rad), at a flow rate of 30 μl/min (flow time, 200 s). The chip surface was deactivated using ProteOn ethanolamine (Bio-Rad) at a flow rate of 30 μl/min. GRFT-glycoprotein interactions were analyzed using 20, 15, 10, 5, 2.5, 1.25, and 0.625 nM GRFT diluted in running buffer with 0.01% Tween and injected at a flow rate of 100 μl/min (flow time, 160 s; time for dissociation, 600 s). The surface was regenerated with ProteOn glycine buffer (Bio-Rad) at 100 μl/min for 18 s. For each glycoprotein, all concentrations were analyzed in duplicate in two independent experiments for a total of four replicates.

(v) Immunohistochemical assay. We performed the immunohistochemical assay as previously described by Nicola et al. (24). Vero cells were seeded into 100 μl of medium in white opaque 96-well plates (1 × 10⁴ cells/well) and incubated overnight at 37°C in a 5% CO$_2$ atmosphere with 98% humidity. Dilutions of GRFT, recombinant HSV-2 glycoprotein D produced in a baculovirus system (N-glycosylated gD; generously provided by Gary H. Cohen and Roselyn J. Eisenberg of the University of Pennsylvania), and recombinant HSV-2 glycoprotein D produced in *Escherichia coli* (nonglycosylated gD; MyBiosource) were prepared in DMEM containing 5% FBS and 1% penicillin-streptomycin. Dilutions were prepared such that the molecular ratio of gD/GRFT was approximately 1:1. Treatments with GRFT, N-glycosylated gD, nonglycosylated gD, N-glycosylated gD-GRFT, and nonglycosylated gD-GRFT involved preincubation at 37°C in a 5% CO$_2$ atmosphere with 98% humidity for 0.5 h. Samples and the microplate containing Vero cell monolayers were prechilled, and then the cells were treated with 25 μl of sample for 1.5 h at 4°C. Fifty microliters of HSV-2 G (4 × 10³ PFU/ml) was added to all wells (except wells with cell controls, which received 50 μl of medium), incubated for an additional 1.5 h at 4°C, and then transferred to 37°C in a 5% CO$_2$ atmosphere with 98% humidity overnight (~18 h). HSV-2 infection was detected using anti-HSV-2 antibody ab9534 (Abcam) and a Histostain-Plus kit (Life Technologies).

GRFT MOA against HPV PsV. (i) Inhibition of HPV PsV adsorption. The assay used to determine the inhibition of HPV PsV adsorption was performed as described above for HSV-2, but the luciferase assay was used (10, 12). For time-of-addition experiments, different concentrations of CG or GRFT were added at time 0 h, 2 h, 7 h, 11 h, or 24 h, with time zero representing the time of initial HPV16 PsV inoculation. The luciferase assay was performed under three different conditions of incorporation of CG or GRFT to explore whether GRFT binds to HPV or virus cell receptors: (i) CG or GRFT was added to the cells before they were washed 3 times and HPV16 PsV was added, (ii) CG or GRFT was mixed with HPV16 PsV and the mixture was incubated before it was added to the cells, or (iii) CG or GRFT was added to the cells immediately before the mixture was added to HPV16 PsV.

(ii) Effect of GRFT on α$_6$ integrin expression on HeLa cells. HeLa cells were seeded in 96-well microplates (10⁴ cells/well) in 100 μl of medium and incubated overnight at 37°C in a 5% CO$_2$ atmosphere with 98% humidity. GRFT (0, 4, 20, and 100 μg/ml) was added to the microplates (50 μl per well, six replicates per condition) under the following conditions: (i) it was added to chilled cells and the mixture was incubated at 4°C for 15 min, 2 h, or 7 h (without washing), (ii) it was added to cells and the mixture was incubated at 37°C for 15 min, 2 h, or 7 h (without washing), (iii) it was added to chilled cells and the mixture was incubated at 4°C for 2 h before the cells were washed 3 times with cold medium and incubated at 4°C for an additional 15 min, 2 h, or 7 h, or (iv) it was added to the cells and the mixture was incubated at 37°C for 2 h before the cells were washed 3 times with medium and incubated at 37°C for an additional 15 min, 2 h, or 7 h. The cells were trypsinized for flow cytometry staining. Cells were stained with the live/dead discriminator Aqua (Life Technologies) and incubated for 20 min at 4°C with a phycoerythrin-conjugated anti-integrin α$_6$ MAb (GoH3; 0.1 μg/well; Abcam, Cambridge, MA) diluted in PBS, 5% FBS, and 0.09% sodium azide. Cells were fixed in 2% paraformaldehyde for 10 min at 4°C and analyzed with a BD LSRII flow cytometer. A total of 50,000 events per sample were acquired, and the results analyzed with FlowJo software (v9).

***In vivo* antiviral activity in murine models.** We followed the guidelines of the Animal Welfare Act (25) and the *Guide for the Care and Use of Laboratory Animals* (26). Rockefeller University's Institutional Animal Care and Use Committee (IACUC) of the Comparative Bioscience Center (CBC) approved the animal protocols. Veterinarians at CBC regularly monitored the animals to minimize any distress or pain.

(i) HSV-2 murine model. A vaginal high-HSV-2-dose challenge was performed as previously described (21).

(ii) HPV16 PsV murine model. In assays with the HPV16 PsV murine model, we followed the procedure described by Kizima et al. (10) and Rodriguez et al. (12), adding 50 μl of GRFT solution (19.1 mg/ml) or PBS intravaginally immediately before and 0.5 h after challenge with 8 × 10⁶ copies/10 μl of HPV16 PsV. To assess the activity of the GRFT-CG combination, 20 μl of GRFT-CG or CG gel (12) was added 8 h before HPV16 PsV challenge. *In vivo* luciferase expression was measured as described before (10, 12), but imaging was performed using an IVIS spectrum imaging system (PerkinElmer, Waltham, MA).

Data analyses. The 50% cytotoxic concentrations and EC$_{50}$s were calculated using a dose-response-inhibition analysis with GraphPad Prism (v5.0c) software. The SPR data were analyzed using the kinetic Langmuir model with ProteOn Manager software (Bio-Rad). Statistical analysis for comparison of treatments in the HSV-2 immunohistochemical assay and HPV murine model was performed using the Mann-Whitney U test ($P <$ 0.05). Fisher's exact test was used for comparison of mouse infection after challenge with HSV-2.

RESULTS

The GRFT-CG combination results in better *in vitro* antiviral activity against HSV-2 and HPV than either compound alone. We first investigated GRFT's anti-HPV activity *in vitro*, comparing it with the known anti-HSV-2 and anti-HIV-1 activities. Although the EC$_{50}$s for HPV were higher, we obtained the first evidence that GRFT possesses anti-HPV activity *in vitro* (Fig. 1): the EC$_{50}$ for HPV16 PsV was 35.1 μg/ml (1.39 μM), the EC$_{50}$ for HPV18 PsV was 10.8 μg/ml (0.428 μM), and the EC$_{50}$ for HPV45 PsV was 23.4 μg/ml (0.928 μM), whereas the EC$_{50}$ for HSV-2 was 5.8 μg/ml (230 nM) and the EC$_{50}$ for HIV was at a subnanomolar level (EC$_{50}$ for HIV-1$_{ADA-M}$, 2.3 ng/ml [0.09 nM]; EC$_{50}$ for HIV-1$_{MN}$, 0.88 ng/ml [0.03 nM]). GRFT's anti-HSV-2 activity was also demonstrated by flow cytometry in HeLa cells, with 4 μg/ml GRFT inhibiting ~77% of the infections and 20 and 100 μg/ml GRFT inhibiting ~83% of the infections (see Fig. S1 in the supplemental material). The decrease in ICP-8 expression suggests
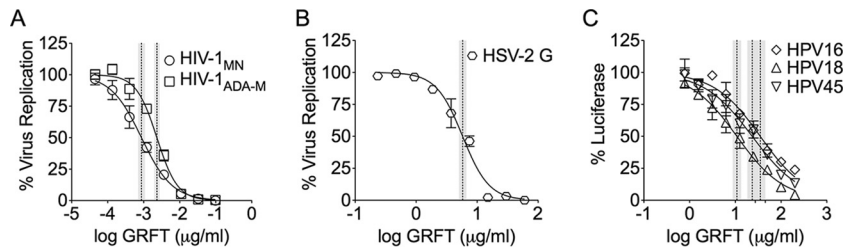
FIG 1 GRFT interference with infection as a measure of activity against HIV (A), HSV (B), and HPV (C). We determined antiviral activity using the TZM-bl cell assay for anti-HIV-1 activity and the luciferase assay (HeLa cells) for anti-HPV16 PsV activity. The dye uptake assay (with PrestoBlue) was used to test the *in vitro* susceptibility of HSV-2 in Vero cells. The graphs show the percent virus replication or reporter gene expression (mean ± SD) relative to that for the virus control (triplicate assays were performed per condition). The dotted and shaded vertical lines represent the EC_{50}s with their 95% confidence intervals.

antiviral activity in a single viral cycle at a high MOI. The GRFT-CG combination reduced the EC_{50}s compared to the EC_{50} of either GRFT or CG alone for both HSV-2 (82.1% and 70.4% reductions, respectively) and HPV16 (68.4% and 71.3% reductions, respectively) (Table 1).

GRFT blocks HSV-2 or HPV postadsorption events. We performed a temperature-dependent assay where cells are exposed to virus in the presence of various concentrations of GRFT at 4°C to investigate if GRFT could block viral infection by preventing the initial attachment to cells. The results showed that no inhibition of HSV-2 or HPV PsV (Fig. 2A) infection was seen under these conditions, prompting us to test if GRFT has postattachment inhibitory effects on HSV-2 and/or HPV PsV infectivity. Using a simple temperature shift experiment, where the HSV-2 inoculum is inactivated if entry is prevented, we observed inhibition of HSV-2 entry by GRFT (Fig. 2B). In order to test postattachment antiviral activity against HPV PsV, we performed a time course experiment in which cells were exposed to different concentrations of GRFT at different times after HPV PsV addition, using as a control differ-

TABLE 1 GRFT-CG combination increases the antiviral activity against HSV-2 and HPV16

Virus and compound(s)	EC_{50} (95% confidence interval)	% EC_{50} reduction
HSV-2		
GRFT	19 µg/ml (16.1–22.4)	NA^a
CG	11.5 ng/ml (9.7–13.6)	NA
CG-GRFT	3.4 ng/ml (2.3–4.9)^b	70.4^c
CG-GRFT	3.4 µg/ml (2.3–4.9)^d	82.1^e
HPV16		
GRFT	35.1 µg/ml (27.3–45.1)	NA
CG	38.6 ng/ml (30.8–48.4)	NA
CG-GRFT	11.1 ng/ml (8.5–14.4)^b	71.3^c
CG-GRFT	11.1 µg/ml (8.5–14.4)^d	68.4^e

^{a} NA, not applicable.
^{b} The EC_{50}s for the combinations are based on the CG concentration or are in comparison to the EC_{50} of CG alone.
^{c} The percent EC_{50} reduction values for the combinations are based on the CG concentration or are in comparison to the EC_{50} of CG alone. Percent EC_{50} reduction = [1 − (combination EC_{50}/CG IC_{50})] × 100, where IC_{50} is the 50% inhibitory concentration.
^{d} The EC_{50}s for the combinations are based on the GRFT concentration or are in comparison to the EC_{50} of GRFT alone.
^{e} The percent EC_{50} reduction values for the combinations are based on the GRFT concentration or are in comparison to the EC_{50} of GRFT alone. Percent EC_{50} reduction = [1 − (combination EC_{50}/GRFT IC_{50})] × 100, where IC_{50} is the 50% inhibitory concentration.

ent concentrations of CG. Figure 2C shows that GRFT and CG were able to block HPV PsV infection even when these compounds were added 11 h after HPV PsV was added to the cells. The results demonstrate that although GRFT failed to prevent HPV PsV attachment, its activity in this assay was consistent with the prevention of HPV postadsorption events and indicates that GRFT must be acting at a late step in the HPV entry process.

GRFT binds to gD to block HSV-2 infection. In order to study if GRFT blocks HSV-2 infection by targeting gD, we performed experiments to first prove that GRFT binds to gD and then determined that GRFT interferes with gD binding to cellular receptors. The Western blot assay showed GRFT binding to HSV-2 G purified/lysed virus particles (Fig. 2D) by the presence of a band in the gD position (52 kDa) (27) but also very strong bands for other glycoproteins that contain N-glycosylation. This was corroborated by immunoprecipitation, where strong bands were identified with anti-gB and anti-gD (Fig. 2E) but not with anti-gH or anti-gL (data not shown). GRFT binds very tightly to gp120 derived from HIV R5, as seen by the low equilibrium dissociation constant (K_D) (Table 2). The tight binding appears to derive from a high on rate with a high association rate constant (k_a) and a low off rate with a low dissociation rate constant (k_d) (Table 2). The binding kinetics for gD derived from the HSV-2 G strain were only slightly different from those for gp120 (Table 2). Further support that GRFT targets gD to prevent HSV-2 infection was obtained by demonstrating that an equimolar combination of GRFT and soluble glycosylated (but not nonglycosylated) gD significantly impeded ($P < 0.0087$) each other's antiviral properties (Fig. 2F).

GRFT induces internalization of the HPV secondary receptor and reduces HPV PsV infection in the murine model. The anti-HPV effects of GRFT could be due to either direct binding to HPV PsV or binding to cellular receptors that mediate postattachment steps. GRFT did not block HPV infection by neutralizing HPV16 PsV, since SPR did not show binding of GRFT to HPV16 PsV (data not shown). Infection experiments were set up to explore this further by preincubating cells or virus with GRFT. GRFT blocked HPV PsV infection when it was preincubated with virus or added simultaneously to cells without washing the inoculum or compound, but it failed to provide protection when it was first added to cells followed by a washing step (Fig. 3A). This finding suggests that GRFT did not simply block a cell surface receptor to neutralize infection. To explore whether GRFT triggers HPV receptor internalization, we preincubated HeLa cells with GRFT at 4°C or 37°C, followed or not by washing, reculture, and monitoring of the expression of α_6 (an HPV secondary receptor) on the HeLa cell surface over time. At 4°C, α_6 expres-
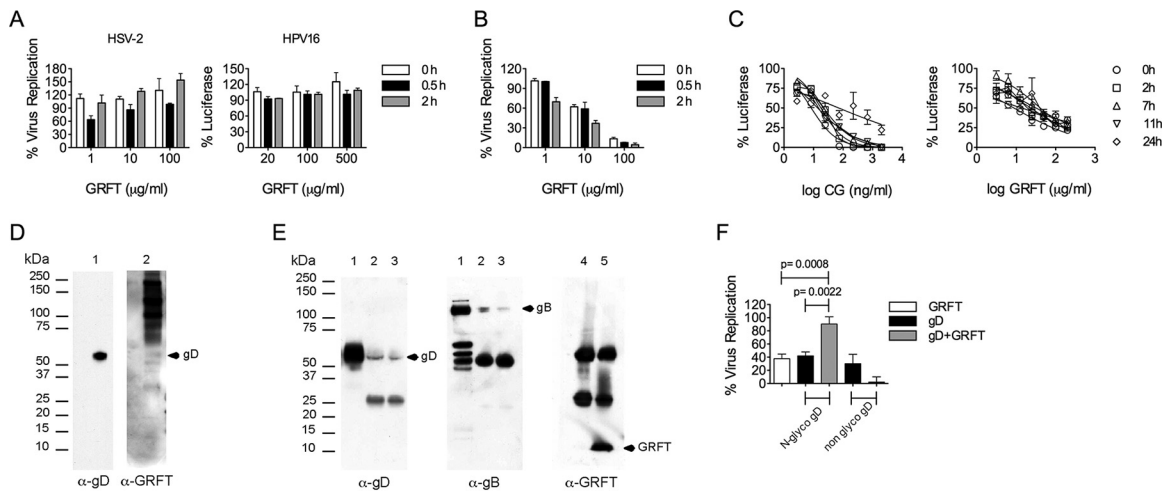
FIG 2 GRFT prevents HSV-2 and HPV postadsorption events. (A) HSV-2 G or HPV16 PsV and different concentrations of GRFT or medium (virus control) were preincubated for 0 h, 0.5 h, and 2 h at 37°C before being added to prechilled Vero cells (for HSV-2) or HeLa cells (for HPV16 PsV) and kept at 4°C for 2 h. The cells were washed 3 times before addition of the overlay and incubation at 48 h and 37°C in a 5% CO_2 atmosphere with 98% humidity. Finally, the cells were fixed and stained prior to counting the numbers of PFU. (B) The same as in panel A for HSV-2, but after 2 h of incubation at 4°C, the cells were switched to 37°C for an additional 2 h, followed by a 2-min treatment with citric acid buffer (pH 3.0). (C) Different concentrations of CG or GRFT were added at the indicated time points, with time zero representing the time of initial HPV16 PsV inoculation. The graph shows the percent reporter gene expression (mean ± SD) relative to that for the virus control (triplicate assays were performed per condition). (D) Western blot of purified HSV-2 lysate. Membranes were incubated overnight at 4°C with mouse anti-gD MAb DL11 (lane 1) or 1 μg/ml GRFT (lane 2). The membranes were washed and incubated for 1 h at room temperature with HRP-conjugated anti-mouse Ig (lane 1) or were incubated overnight at 4°C with rabbit anti-GRFT antibody (lane 2), before being washed and incubated with HRP-conjugated anti-rabbit immunoglobulin antibody (1 h at room temperature). (E) HSV-2-infected Vero cells were lysed, preincubated with GRFT, and immunoprecipitated with anti-GRFT antibody. Lanes 1, cell lysate without immunoprecipitation; lanes 2, HeLa cell lysate 24 h after HSV-2 infection with immunoprecipitation in the presence of GRFT and anti-GRFT antibody; lanes 3, same as lanes 2 but 48 h after HSV-2 infection; lanes 4 and 5, immunoprecipitation controls without and with GRFT, respectively. In the experiments described in the legends to panels D and E, the membranes were processed using an ECL Western blotting detection system to capture the bands on X-ray films. A representative blot of three repeats is shown. (F) Soluble GRFT, N-glycosylated (N-glyco), nonglycosylated gD, or a mixture of N-glycosylated and nonglycosylated gD-GRFT was preincubated before addition to Vero cells. HSV-2 G was then added, and infection was detected by an immunohistochemical assay after overnight incubation. Statistical analysis was performed using the Mann-Whitney U test ($P < 0.05$). The graphs show the percent virus replication (mean ± SD) relative to that for the virus control (2 to 4 independent experiments with duplicate experiments per condition).

sion remained constant over time with or without the washing step, but incubation at 37°C dramatically decreased the level of α_6 integrin expression (Fig. 3B). HeLa cells preincubated with GRFT at 500 μg/ml at 37°C followed by a washing step showed a decrease in the level of α_6 expression only at 15 min after GRFT was washed out. This may represent a process of recovery of α_6 expression, since normal levels were reached at 2 h after GRFT was washed out.

The GRFT-CG combination reduces HSV-2 and HPV infections *in vivo*. Finally, we set out to determine if the GRFT-CG combination was more effective than either component alone against HSV-2 and HPV *in vivo*, as we had seen *in vitro* (Table 1). We used stringent, high-virus-dose models in which medroxyprogesterone acetate (Depo-Provera)-treated mice were challenged vaginally with 10^6 PFU of HSV-2 or 8×10^6 copies/10 μl of HPV16 PsV after applying each compound alone (1.9% GRFT or 3% CG) or in combination (0.1% GRFT plus 3% CG). Under

these conditions, GRFT or CG alone afforded minimal protection against HSV-2, but GRFT-CG applied 10 min or 1 h before virus challenge significantly reduced the level of HSV-2 infection ($P = 0.0352$ relative to the results for the CG or GRFT controls given 10 min prior to challenge; Fig. 4A). Supporting GRFT's moderate EC_{50} against HPV and its potential MOA (see above), GRFT significantly protected mice against vaginal HPV infection when dosed during and after HPV16 pseudovirus challenge ($P < 0.026$ relative to the results for the HEC placebo), but much greater protection was afforded by CG alone for up to 8 h ($P = 0.0022$ relative to the results for the HEC placebo) (Fig. 4B), and an additive effect of GRFT and CG could not be determined. Thus, the potent activity of CG in this model masked any additional anti-HPV effect of GRFT. Together these data support the potential of the GRFT-CG formulation to prevent HSV-2 and HPV infection.

DISCUSSION

Herein we describe how GRFT may block HSV-2 infection and also report for the first time that GRFT has anti-HPV activity. We propose that the combination of GRFT and CG be used to increase the antiviral activity of GRFT against both viruses. It has been suggested that GRFT might block HSV-2 infection mainly by preventing cell-to-cell spread (7). While it may be true, our experiments suggest that entry inhibition plays an important and additional role in the MOA of GRFT against HSV-2.

TABLE 2 GRFT binds HSV-2 gD but with a lower affinity than HIV gp120[a]

HIV-1 gp120			HSV-2 gD		
k_a ($M^{-1} s^{-1}$)	k_d (s^{-1})	K_D (M)	k_a ($M^{-1} s^{-1}$)	k_d (s^{-1})	K_D (M)
2.19×10^6	1.75×10^{-3}	7.98×10^{-10}	2.56×10^6	4.52×10^{-3}	1.76×10^{-9}

[a] The analyte was GRFT. For each glycoprotein, all concentrations were analyzed in duplicate in two independent experiments.
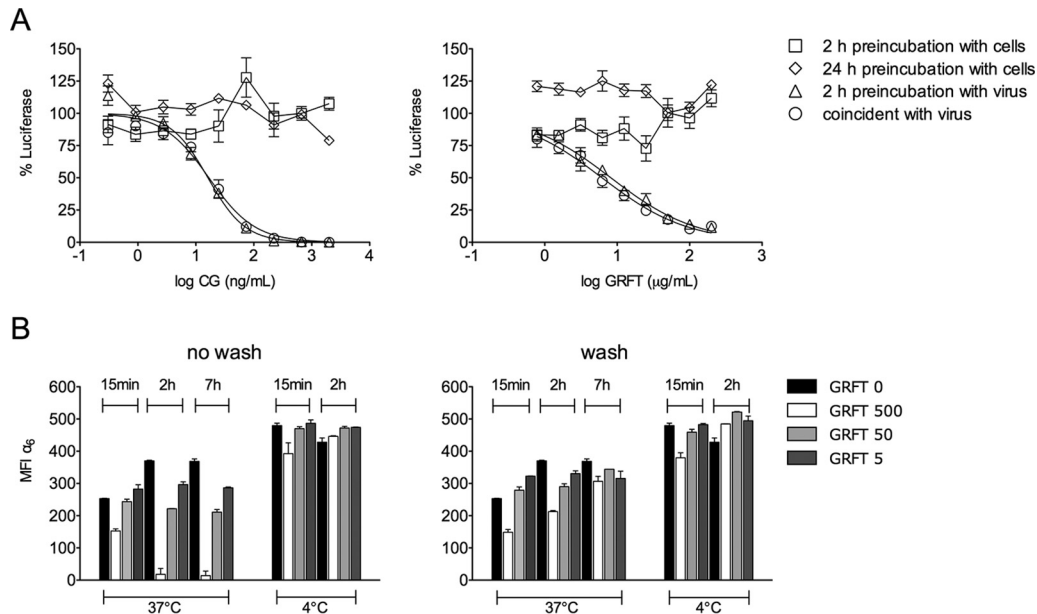
FIG 3 GRFT blocks HPV16 PsV infection by inducing HPV secondary receptor internalization in HeLa cells. (A) Different concentrations of CG or GRFT were administered under the following conditions: (i) CG or GRFT was added to HeLa cells for 2 h (squares) or 24 h (diamonds) at 37°C before the cells were washed 3 times and HPV16 PsV was added, (ii) CG or GRFT was mixed with HPV16 PsV and the mixture was incubated for 2 h at 37°C before addition to cells (triangles), or (iii) CG or GRFT was added to cells immediately before addition to HPV16 PsV (circles). The graphs show the percent reporter gene expression (mean ± SD) relative to that for the virus control (triplicate assays were performed per condition). (B) α_6 integrin expression on the HeLa cell surface was analyzed under the following conditions: (i) CG or GRFT was added to the mixture was incubated at 4°C for 2 h before the cells were washed 3 times with cold medium and incubated at 4°C for 15 min, 2 h, or 7 h, (ii) CG or GRFT was added to cells and the mixture was incubated at 37°C for 2 h before the cells were washed 3 times with medium and incubated at 37°C for 15 min, 2 h, or 7 h, (iii) CG or GRFT was added to chilled cells without washing and the mixture was incubated at 4°C for 15 min, 2 h, or 7 h, or (iv) CG or GRFT was added to cells without washing and the mixture was incubated at 37°C for 15 min, 2 h, or 7 h. The results represent the mean ± SEM from two independent experiments with pooling of data from six replicate experiments per condition for anti-α_6 staining and flow cytometry analyses. MIF, mean fluorescence intensity.

Similar to the findings of previous studies with HIV, our data suggest that GRFT may interfere with HSV-2 entry. This MOA is similar to that described in previous studies on GRFT's activity against HIV, which showed inhibition of viral entry but not attachment ([3]). HSV-2 entry is governed by four glycoproteins (gD,

gB, gH, and gL) while viral adsorption (which is unaffected by GRFT) involves two glycoproteins (gC and gB).

We concentrated our attention on glycoproteins that may support the primary cell-to-cell spread MOA of HSV-2 inhibition by GRFT proposed by Nixon et al. ([7]) as well as entry inhibition (also
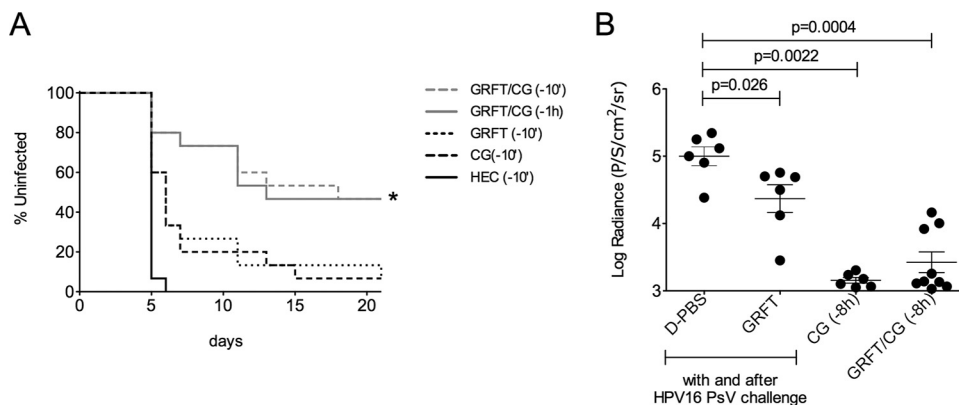

FIG 4 The GRFT-CG combination significantly reduced HSV-2 and HPV16 PsV infection in murine models. (A) Medroxyprogesterone acetate-treated BALB/c mice were given CG, GRFT, or HEC formulations intravaginally at 10 min before HSV-2 challenge or GRFT-CG 10 min or 1 h after HSV-2 challenge ($n = 15$ mice per treatment group). The percentages of uninfected animals over time, based on symptoms, are shown for each treatment group. *, $P < 0.05$ versus GRFT and CG, Fisher's exact test. (B) Medroxyprogesterone acetate-treated BALB/c mice were given CG intravaginally at 8 h before HPV16 PsV challenge or GRFT during and 1 h after HPV16 PsV challenge ($n = 6$ to 9 mice per treatment group). In vivo luciferase expression was detected using an IVIS Spectrum imaging system and is expressed as the mean luminescence in numbers of photons per second per cm² per steradian (P/S/cm²/sr) ± SD for each animal. Statistical analysis was performed using the Mann-Whitney U test ($P < 0.05$). D-PBS, Dulbecco's phosphate-buffered saline.

mentioned by Nixon et al. for the MOA of GRFT [7] and supported by the work herein). HSV gD is essential not only for viral entry but also for cell-to-cell spread. Different HSV-1 mutants lacking either the gD gene (28) or N-linked glycosylation in gD cannot spread between cells (29, 30). Furthermore, the fact that the cell-to-cell spread of wild-type HSV is reduced in cells that lack the ability to add mannose-6-phosphate residues to glycoproteins (29) also supports an important role for gD glycosylation in the cell-to-cell spread of HSV-2. Glycoprotein gD seems to be of particular importance in explaining the MOA of GRFT since it participates in both viral entry and cell-to-cell spread. Glycoprotein B participates in viral entry and cell-to-cell spread (31), but it also plays a major role in viral adsorption, although this step was not inhibited by GRFT in our experiments. However, our immunoprecipitation results show that binding to other HSV-2 glycoproteins (like gB) may contribute to the antiviral activity of GRFT.

We also exploited the ability of soluble gD to interact in *cis* with the gD receptor and make it unavailable to HSV virions (32–36). GRFT interferes with the antiviral properties of soluble gD, suggesting that GRFT-gD binding inhibits the critical role that gD plays in HSV-2 entry. The interaction of gD with receptors requires the native structure but not the N-glycosylation of gD (37) (we showed HSV-2 inhibition by both glycosylated and nonglycosylated gD). Additionally, gD N-glycosylation sites are close to the gD functional domains for binding of the gD receptor (38). Therefore, GRFT-gD binding may occlude the receptor contact site of gD and block the binding of gD to the receptor.

The SPR results showed only a slight difference in the affinities of gD and gp120 for GRFT and therefore cannot explain the remarkable difference in the antiviral activities seen in the *in vitro* antiviral assays, in which the EC_{50}s were about 10,000-fold lower for anti-HIV activity than anti-HSV-2 activity. A possible explanation could be that while HIV contains approximately only 10 gp120 trimers per virion, HSV-2 virions have about 300 gD molecules that need to be neutralized by GRFT. It has been shown that every single gD molecule in the HSV-2 virion must be neutralized in order to block HSV-2 infection (39). Additionally, GRFT binding to other HSV-2 structural glycoproteins that may or may not contribute to the antiviral activity but that may still sequester GRFT from binding to gD may explain why so much GRFT is required to block HSV-2 infection compared to the amount of GRFT required for inhibition of HIV.

We also tested GRFT's antiviral activity against the nonenveloped virus HPV. HPV's cycle of replication starts with adsorption to cells followed by a lag (several hours) where conformational changes mediated by host factors increase L2 N-terminus exposure. These conformational changes allow the virion to interact with the secondary receptor (α_6 integrin) and to enter the target cell (40). Like CG (9), GRFT can block HPV postbinding events (even when GRFT is added several hours after addition of HPV16 PsV), and this inhibition is not achieved when HeLa cells are preincubated with GRFT for several hours followed by a washout. The fact that GRFT could block HPV, a naked virus, is very intriguing. There was no GRFT binding to HPV16 PsV by SPR (data not shown) in our experiments, prompting us to explore a possible effect of GRFT on α_6 integrin (described to be an HPV secondary receptor in basal keratinocytes) (41, 42). The addition of GRFT to HeLa cells resulted in α_6 internalization. Our experiments suggest that GRFT inhibits HPV by targeting α_6 integrin, but it is still possible that the HPV-integrin-GRFT complex could

be internalized without leading to infection. The integrin internalization after GRFT binding is not surprising, since binding of other molecules to α_6 has been shown to trigger internalization (43, 44). This result, together with the partial inhibition of HPV16 PsV in the murine model, may suggest the need for the sustained presence of GRFT in order to achieve better *in vivo* anti-HPV activity as well as combination of GRFT with a more potent anti-HPV agent, like CG. While CG's activity against HPV dominated in the CG-GRFT mix, the benefits of the use of this combination were supported by the significant decrease in HSV-2 infection ($P = 0.0352$) in the murine model compared to the decrease achieved by the use of CG or GRFT alone. Additionally, the inclusion of GRFT in this combination is key to obtain potent anti-HIV activity and achieve a broad spectrum of activity against three relevant viruses responsible for STIs.

The results outlined herein underscore the advantages of combining GRFT with CG for broad antiviral activity against HSV-2 and HPV. We can add to this broad antiviral activity against STIs the previously described antiviral properties of GRFT against HIV and hepatitis C virus (1, 3, 6, 8, 45–47). Our experiments suggest that gD is a target for the anti-HSV properties of GRFT. Interestingly, GRFT seems to target viral entry in enveloped viruses, adding more evidence to an expanding research base on the role of N-glycosylation in viral entry and the coincident susceptibility to antiviral lectins. Finally, not only do we demonstrate for the first time GRFT activity against HPV but we also describe a possible MOA, secondary HPV receptor internalization. Taken together, our results strongly support the development of the GRFT and CG combination as a multipurpose prevention technology.

REFERENCES

1. O'Keefe BR, Vojdani F, Buffa V, Shattock RJ, Montefiori DC, Bakke J, Mirsalis J, d'Andrea AL, Hume SD, Bratcher B, Saucedo CJ, McMahon JB, Pogue GP, Palmer KE. 2009. Scaleable manufacture of HIV-1 entry inhibitor griffithsin and validation of its safety and efficacy as a topical microbicide component. Proc Natl Acad Sci U S A **106:**6099–6104. http://dx.doi.org/10.1073/pnas.0901506106.

2. Huskens D, Schols D. 2012. Algal lectins as potential HIV microbicide candidates. Mar Drugs **10:**1476–1497. http://dx.doi.org/10.3390/md10071476.

3. Alexandre KB, Gray ES, Pantophlet R, Moore PL, McMahon JB, Chakauya E, O'Keefe BR, Chikwamba R, Morris L. 2011. Binding of the mannose-specific lectin, griffithsin, to HIV-1 gp120 exposes the CD4-binding site. J Virol **85:**9039–9050. http://dx.doi.org/10.1128/JVI.02675-10.

4. Moulaei T, Shenoy SR, Giomarelli B, Thomas C, McMahon JB, Dauter Z, O'Keefe BR, Wlodawer A. 2010. Monomerization of viral entry inhibitor griffithsin elucidates the relationship between multivalent binding to carbohydrates and anti-HIV activity. Structure **18:**1104–1115. http://dx.doi.org/10.1016/j.str.2010.05.016.

5. Barton C, Kouokam JC, Lasnik AB, Foreman O, Cambon A, Brock G, Montefiori DC, Vojdani F, McCormick AA, O'Keefe BR, Palmer KE. 2014. Activity of and effect of subcutaneous treatment with the broad-spectrum antiviral lectin griffithsin in two laboratory rodent models. An-

timicrob Agents Chemother **58**:120–127. http://dx.doi.org/10.1128/AAC.01407-13.

6. **Kouokam JC, Huskens D, Schols D, Johannemann A, Riedell SK, Walter W, Walker JM, Matoba N, O'Keefe BR, Palmer KE.** 2011. Investigation of griffithsin's interactions with human cells confirms its outstanding safety and efficacy profile as a microbicide candidate. PLoS One **6**:e22635. http://dx.doi.org/10.1371/journal.pone.0022635.

7. **Nixon B, Stefanidou M, Mesquita PM, Fakioglu E, Segarra T, Rohan L, Halford W, Palmer KE, Herold BC.** 2013. Griffithsin protects mice from genital herpes by preventing cell-to-cell spread. J Virol **87**:6257–6269. http://dx.doi.org/10.1128/JVI.00012-13.

8. **Takebe Y, Saucedo CJ, Lund G, Uenishi R, Hase S, Tsuchiura T, Kneteman N, Ramessar K, Tyrrell DL, Shirakura M, Wakita T, McMahon JB, O'Keefe BR.** 2013. Antiviral lectins from red and blue-green algae show potent in vitro and in vivo activity against hepatitis C virus. PLoS One **8**:e64449. http://dx.doi.org/10.1371/journal.pone.0064449.

9. **Buck CB, Thompson CD, Roberts JN, Muller M, Lowy DR, Schiller JT.** 2006. Carrageenan is a potent inhibitor of papillomavirus infection. PLoS Pathog **2**:e69. http://dx.doi.org/10.1371/journal.ppat.0020069.

10. **Kizima L, Rodriguez A, Kenney J, Derby N, Mizenina O, Menon R, Seidor S, Zhang S, Levendosky K, Jean-Pierre N, Pugach P, Villegas G, Ford BE, Gettie A, Blanchard J, Piatak M, Jr, Lifson JD, Paglini G, Teleshova N, Zydowsky TM, Robbiani M, Fernandez-Romero JA.** 2014. A potent combination microbicide that targets SHIV-RT, HSV-2 and HPV. PLoS One **9**:e94547. http://dx.doi.org/10.1371/journal.pone.0094547.

11. **Roberts JN, Buck CB, Thompson CD, Kines R, Bernardo M, Choyke PL, Lowy DR, Schiller JT.** 2007. Genital transmission of HPV in a mouse model is potentiated by nonoxynol-9 and inhibited by carrageenan. Nat Med **13**:857–861. http://dx.doi.org/10.1038/nm1598.

12. **Rodriguez A, Kleinbeck K, Mizenina O, Kizima L, Levendosky K, Jean-Pierre N, Villegas G, Ford BE, Cooney ML, Teleshova N, Robbiani M, Herold BC, Zydowsky T, Fernandez Romero JA.** 2014. In vitro and in vivo evaluation of two carrageenan-based formulations to prevent HPV acquisition. Antiviral Res **108**:88–93. http://dx.doi.org/10.1016/j.antiviral.2014.05.018.

13. **Whitehead SJ, McLean C, Chaikummao S, Braunstein S, Utaivoravit W, van de Wijgert JH, Mock PA, Siraprapasiri T, Friedland BA, Kilmarx PH, Markowitz LE.** 2011. Acceptability of Carraguard vaginal microbicide gel among HIV-infected women in Chiang Rai, Thailand. PLoS One **6**:e14831. http://dx.doi.org/10.1371/journal.pone.0014831.

14. **Carraguard Phase II South Africa Study Team.** 2010. Expanded safety and acceptability of the candidate vaginal microbicide Carraguard® in South Africa. Contraception **82**:563–571. http://dx.doi.org/10.1016/j.contraception.2010.04.019.

15. **Martin S, Blanchard K, Manopaiboon C, Chaikummao S, Schaffer K, Friedland B, Kilmarx PH.** 2010. Carraguard acceptability among men and women in a couples study in Thailand. J Womens Health (Larchmt) **19**:1561–1567. http://dx.doi.org/10.1089/jwh.2009.1362.

16. **Skoler-Karpoff S, Ramjee G, Ahmed K, Altini L, Plagianos MG, Friedland B, Govender S, De Kock A, Cassim N, Palanee T, Dozier G, Maguire R, Lahteenmaki P.** 2008. Efficacy of Carraguard for prevention of HIV infection in women in South Africa: a randomised, double-blind, placebo-controlled trial. Lancet **372**:1977–1987. http://dx.doi.org/10.1016/S0140-6736(08)61842-5.

17. **Marais D, Gawarecki D, Allan B, Ahmed K, Altini L, Cassim N, Gopolang F, Hoffman M, Ramjee G, Williamson AL.** 2011. The effectiveness of Carraguard, a vaginal microbicide, in protecting women against high-risk human papillomavirus infection. Antivir Ther **16**:1219–1226. http://dx.doi.org/10.3851/IMP1890.

18. **Zacharopoulos VR, Phillips DM.** 1997. Vaginal formulations of carrageenan protect mice from herpes simplex virus infection. Clin Diagn Lab Immunol **4**:465–468.

19. **Maguire RA, Zacharopoulos VR, Phillips DM.** 1998. Carrageenan-based nonoxynol-9 spermicides for prevention of sexually transmitted infections. Sex Transm Dis **25**:494–500. http://dx.doi.org/10.1097/00007435-199810000-00010.

20. **Carlucci MJ, Ciancia M, Matulewicz MC, Cerezo AS, Damonte EB.** 1999. Antiherpetic activity and mode of action of natural carrageenans of diverse structural types. Antiviral Res **43**:93–102. http://dx.doi.org/10.1016/S0166-3542(99)00038-8.

21. **Fernandez-Romero JA, Abraham CJ, Rodriguez A, Kizima L, Jean-Pierre N, Menon R, Begay O, Seidor S, Ford BE, Gil PI, Peters J, Katz D, Robbiani M, Zydowsky TM.** 2012. Zinc acetate/carrageenan gels exhibit potent activity in vivo against high-dose herpes simplex virus 2 vaginal and rectal challenge. Antimicrob Agents Chemother **56**:358–368. http://dx.doi.org/10.1128/AAC.05461-11.

22. **Tien D, Schnaare RL, Kang F, Cohl G, McCormick TJ, Moench TR, Doncel G, Watson K, Buckheit RW, Lewis MG, Schwartz J, Douville K, Romano JW.** 2005. In vitro and in vivo characterization of a potential universal placebo designed for use in vaginal microbicide clinical trials. AIDS Res Hum Retroviruses **21**:845–853. http://dx.doi.org/10.1089/aid.2005.21.845.

23. **Begay O, Jean-Pierre N, Abraham CJ, Chudolij A, Seidor S, Rodriguez A, Ford BE, Henderson M, Katz D, Zydowsky T, Robbiani M, Fernandez-Romero JA.** 2011. Identification of personal lubricants that can cause rectal epithelial cell damage and enhance HIV type 1 replication in vitro. AIDS Res Hum Retroviruses **27**:1019–1024. http://dx.doi.org/10.1089/aid.2010.0252.

24. **Nicola AV, Willis SH, Naidoo NN, Eisenberg RJ, Cohen GH.** 1996. Structure-function analysis of soluble forms of herpes simplex virus glycoprotein D. J Virol **70**:3815–3822.

25. **Code of Federal Regulations.** 2001. Animals and animal products, chapter 1, subchapter A. *In* Animal Welfare Act and Regulation. U.S. Department of Agriculture, Beltsville, MD.

26. **National Research Council.** 2011. Guide for the care and use of laboratory animals, 8th ed. National Academies Press, Washington, DC.

27. **Matthews JT, Cohen GH, Eisenberg RJ.** 1983. Synthesis and processing of glycoprotein D of herpes simplex virus types 1 and 2 in an in vitro system. J Virol **48**:521–533.

28. **Ligas MW, Johnson DC.** 1988. A herpes simplex virus mutant in which glycoprotein D sequences are replaced by beta-galactosidase sequences binds to but is unable to penetrate into cells. J Virol **62**:1486–1494.

29. **Brunetti CR, Burke RL, Hoflack B, Ludwig T, Dingwell KS, Johnson DC.** 1995. Role of mannose-6-phosphate receptors in herpes simplex virus entry into cells and cell-to-cell transmission. J Virol **69**:3517–3528.

30. **Sodora DL, Eisenberg RJ, Cohen GH.** 1991. Characterization of a recombinant herpes simplex virus which expresses a glycoprotein D lacking asparagine-linked oligosaccharides. J Virol **65**:4432–4441.

31. **Cheshenko N, Herold BC.** 2002. Glycoprotein B plays a predominant role in mediating herpes simplex virus type 2 attachment and is required for entry and cell-to-cell spread. J Gen Virol **83**:2247–2255. http://dx.doi.org/10.1099/0022-1317-83-9-2247.

32. **Campadelli-Fiume G, Arsenakis M, Farabegoli F, Roizman B.** 1988. Entry of herpes simplex virus 1 in BJ cells that constitutively express viral glycoprotein D is by endocytosis and results in degradation of the virus. J Virol **62**:159–167.

33. **Campadelli-Fiume G, Qi S, Avitabile E, Foa-Tomasi L, Brandimarti R, Roizman B.** 1990. Glycoprotein D of herpes simplex virus encodes a domain which precludes penetration of cells expressing the glycoprotein by superinfecting herpes simplex virus. J Virol **64**:6070–6079.

34. **Geraghty RJ, Jogger CR, Spear PG.** 2000. Cellular expression of alpha-herpesvirus gD interferes with entry of homologous and heterologous alphaherpesviruses by blocking access to a shared gD receptor. Virology **268**:147–158. http://dx.doi.org/10.1006/viro.1999.0157.

35. **Johnson RM, Spear PG.** 1989. Herpes simplex virus glycoprotein D mediates interference with herpes simplex virus infection. J Virol **63**:819–827.

36. **Martin LB, Montgomery PC, Holland TC.** 1992. Soluble glycoprotein D blocks herpes simplex virus type 1 infection of rat eyes. J Virol **66**:5183–5189.

37. **Whitbeck JC, Peng C, Lou H, Xu R, Willis SH, Ponce de Leon M, Peng T, Nicola AV, Montgomery RI, Warner MS, Soulika AM, Spruce LA, Moore WT, Lambris JD, Spear PG, Cohen GH, Eisenberg RJ.** 1997. Glycoprotein D of herpes simplex virus (HSV) binds directly to HVEM, a member of the tumor necrosis factor receptor superfamily and a mediator of HSV entry. J Virol **71**:6083–6093.

38. **Chiang HY, Cohen GH, Eisenberg RJ.** 1994. Identification of functional regions of herpes simplex virus glycoprotein gD by using linker-insertion mutagenesis. J Virol **68**:2529–2543.

39. **Clarke RW, Drews A, Browne H, Klenerman D.** 2013. A single gD glycoprotein can mediate infection by herpes simplex virus. J Am Chem Soc **135**:11175–11180. http://dx.doi.org/10.1021/ja4038406.

40. **Raff AB, Woodham AW, Raff LM, Skeate JG, Yan L, Da Silva DM, Schelhaas M, Kast WM.** 2013. The evolving field of human papillomavi-

rus receptor research: a review of binding and entry. J Virol **87:**6062–6072. http://dx.doi.org/10.1128/JVI.00330-13.

41. **Evander M, Frazer IH, Payne E, Qi YM, Hengst K, McMillan NA.** 1997. Identification of the alpha6 integrin as a candidate receptor for papillomaviruses. J Virol **71:**2449–2456.

42. **Aksoy P, Abban CY, Kiyashka E, Qiang W, Meneses PI.** 2014. HPV16 infection of HaCaTs is dependent on beta4 integrin, and alpha6 integrin processing. Virology **449:**45–52. http://dx.doi.org/10.1016/j.virol.2013.10.034.

43. **Poumay Y, Leclercq-Smekens M, Grailly S, Degen A, Leloup R.** 1993. Specific internalization of basal membrane domains containing the integrin alpha 6 beta 4 in dispase-detached cultured human keratinocytes. Eur J Cell Biol **60:**12–20.

44. **Gaietta G, Redelmeier TE, Jackson MR, Tamura RN, Quaranta V.** 1994. Quantitative measurement of alpha 6 beta 1 and alpha 6 beta 4 integrin internalization under cross-linking conditions: a possible role for alpha 6 cytoplasmic domains. J Cell Sci **107**(Pt 12)**:**3339–3349.

45. **Mori T, O'Keefe BR, Sowder RC, II, Bringans S, Gardella R, Berg S, Cochran P, Turpin JA, Buckheit RW, Jr, McMahon JB, Boyd MR.** 2005. Isolation and characterization of griffithsin, a novel HIV-inactivating protein, from the red alga Griffithsia sp. J Biol Chem **280:**9345–9353. http://dx.doi.org/10.1074/jbc.M411122200.

46. **O'Keefe BR, Giomarelli B, Barnard DL, Shenoy SR, Chan PK, McMahon JB, Palmer KE, Barnett BW, Meyerholz DK, Wohlford-Lenane CL, McCray PB, Jr.** 2010. Broad-spectrum in vitro activity and in vivo efficacy of the antiviral protein griffithsin against emerging viruses of the family Coronaviridae. J Virol **84:**2511–2521. http://dx.doi.org/10.1128/JVI.02322-09.

47. **Xue J, Hoorelbeke B, Kagiampakis I, Demeler B, Balzarini J, Liwang PJ.** 2013. The griffithsin dimer is required for high-potency inhibition of HIV-1: evidence for manipulation of the structure of gp120 as part of the griffithsin dimer mechanism. Antimicrob Agents Chemother **57:**3976–3989. http://dx.doi.org/10.1128/AAC.00332-13.